Industry Science and Engineering Vol. 1 No. 5, 2024

Research on Ironmaking Technology of the Ming Dynasty in Benxi Area based on Metallurgical-Related Principles

Huang Yan[1,2,3], Chen Ren[1,3], Jiang Maofa[2], Chen Shiyi[2], Sui Yingying[1], Mei Xiaohui[1,2], Jin Jun[4]
[1]*School of Metallurgy and Materials Engineering, Benxi, China*
[2]*Northeastern university School of Metallurgy, Shenyang, China*
[3]*Liaoning Key Laboratory of Optimization and Utilization of Non-associated Low-grade Iron Ore in Benxi, Benxi, China*
[4]*Benxi Museum, Benxi, China*

Abstract: This work carries out physical and chemical analysis of Ming dynasty slag samples, fragments of ironmaking reactor (crucible), and iron agricultural tools (in Benxi Museum) in the Benxi area, and then constructs a ternary phase diagram of slag composition utilizing relevant principles of metallurgy to calculate the soft melting temperature of the slag. The values of smelting temperature are calculated based on slag-metal distribution ratio of sulfur and using the J. F. Elliot's empirical equation, respectively, and are subsequently compared. In addition, adaptation relationship between slag and metal compositions is built based on specific constraint conditions. The results show that the smelting temperature for ironmaking at the historical site ranges from 1300℃ to 1480℃ and the carbon content of the Ming dynasty agricultural tools in Benxi Museum ranges from 0.85% to 4.75%. Applying theories related to refractory materials, it is estimated that the refractoriness of the ironmaking reactor at the site exceeds 1700℃. The carbon and sulfur contents in the Ming dynasty agricultural tools allow for inferences regarding the processing characteristics of iron tools for various applications. Through the analysis of the relationship between blast pressure and smelting temperature, it is deduced that blast equipment was used in the ironmaking process at the site. These results provide a critical theoretical foundation for the investigation of ironmaking technology in northeastern China during the Ming dynasty.

Keywords: Benxi Area; History of Ironmaking; Ming Dynasty; Ironmaking Process; Slag-Metal Distribution Ratio of Sulfur; Adaptation Relationship

The smelting and application of metals marked the turning point in humanity's transition from barbarism to civilization. Archaeology's "Three-Age System" considers the production capability, manufacturing efficiency, and performance level of iron tools as key indicators of the development of productivity in ancient societies, elevating the significance of iron tools to a criterion for defining human civilization. Engels stated, "Iron is the last and most important of the raw materials that have played a revolutionary role in history. " Northeastern China is rich in mineral resources, particularly iron ore in the areas of Benxi, Liaoyang, and Anshan in present-day Liaoning province. These resources were already being extensively exploited during the Liao dynasty's rule over the region. In the Qing dynasty, Benxi was renowned for its mining, earning the region the reputation of being "the Northern counterpart to Hanyang's Hanyeping, " and in modern times, it became known as the "City of Coal and Iron. " With the simultaneous advantages of iron ore and coal resources, the Benxi region became one of the important birthplaces of ironmaking technology in China.

In the study of ironmaking history, the method most commonly used involves analyzing the chemical composition and structure and texture of slag or iron products to infer the production process. Although it is relatively easy to obtain ancient slag, iron products, and artifacts such as reactors from archaeological sites, it is almost impossible to collect all types of evidence—slag, iron, and reactors—simultaneously from the same historical site. As a result, this approach cannot accurately establish a one-to-one correspondence between slag samples and iron products, making it difficult to accurately infer the ironmaking process using existing metallurgical principles. This often leads to temporal and spatial inconsistencies in the research. the present group conducted field investigations of Ming dynasty metallurgical remains in the Benxi region and performed laboratory studies on the metallurgical artifacts. Using experimental data and principles related to metallurgy, a correlation was established between slag and iron compositions, which allows for inferring the characteristics of the ironmaking technology in that period. By unveiling the technical aspects of Ming dynasty ironmaking in the Benxi region and clarifying the technological features of ironmaking sites in northeastern China during the Ming dynasty, this work can provide valuable scientific references for exploring ancient Chinese ironmaking technology, particularly in the northeastern region. Moreover, the investigation of ancient ironmaking technology of Benxi region can elevate ironmaking culture as a cultural hallmark of Benxi, revitalizing and enriching the region's cultural identity.

1. Breif Introduction of the Site

The Wangguan Ironmaking site is a city-level protected unit located in Benxi, Liaoning province. the geographic coordinates are 123º05′E longitude and 41º10′N latitude. the site is situated on the northern slope of Wangguan valley in Shangniu village, Niuxintai sub-district, on the east side of the Taizi river in Benxi. Due to extensive mining in the area, the landscape is irregular and uneven, as shown in Figure 1. During field investigations at the site, a large number of broken clay pots (hereafter referred to as crucibles) and slag fragments were discovered, as illustrated in Figure 2.

According to the Ming dynasty's *Quan Liao Zhi*, there were 25 "Wei" (military administrative units) established in Liaodong. Each Wei, equivalent to a modern "division, " had its own ironmaking sites, with three such sites located in Benxi area. Notably, the Weining battalion in Benxi had an ironmaking site at Baihu office, which governed Wangguan valley at that time. Therefore, it is inferred that this ironmaking site is likely the location of the Baihu office's ironmaking site under the Weining battalion as recorded in historical texts. To date, no in-depth metallurgical archaeological work has been conducted at this site, nor have there been any related studies on its ironmaking technology.

Figure 1. Historical Ironmaking Site of Wangguan

a-remaining of crucible

b-residual slag fragments

Figure 2. Remaining of Crucible and Residual Slag Fragments in Historical Ironmaking Site of Wangguan

2. Sample Preparation and Testing

2.1 Sample Preparation Method

The slag and crucible fragment samples used in this study were all collected from the Ming dynasty Wangguan ironmaking site in Benxi. the iron samples were obtained from iron farming tools unearthed at this site, which are currently housed in Benxi Museum. These tools include shovels, hoes, sickles, and choppers. the collected raw slag, crucible fragments, intact crucibles from the museum, and iron farming tools are shown in Figures 3 to 6. After cleaning and decontaminating the slag and crucible samples, sections with a diameter of 1 cm to 3 cm were cut and cold-mounted for sample preparation. the microstructure of these samples was observed and photographed using a Zeiss (EVO18) scanning electron microscope, and their composition was analyzed using an Oxford Instruments X-Max20 energy dispersive spectrometer. the composition analysis of the slag and crucible samples was performed using a Bruker XRF (D8 ADVANCE) instrument. To avoid damaging the artifacts, the comprehensive analysis of the Ming dynasty iron farming tools from Benxi Museum was conducted using a SciAps X-200 handheld XRF analyzer, which performed non-destructive testing on the exposed metal surfaces free from rust.

Figure 3. Bulk Slag

Figure 4. Crucible Residual Fragment

Figure 5. Intact Ming Dynasty Crucibles from Benxi Museum

a-shovel

b-hoe

c-sickle

d-chopper

Figure 6. Ming Dynasty Iron Farming Tools

2.2 Composition and Analysis of Slag Samples

The raw bulk slag samples collected from the site were measured and found to have a roughly "bowl-shaped" morphology, corresponding in appearance to the crucible fragments. the density of the slag samples was 1.6389 g/cm³. Table 1 shows the comprehensive analysis results of the slag sample composition.

Table 1. Analysis Results of Slag Samples from the Historical Site

	F	Na_2O	MgO	Al_2O_3	SiO_2	P_2O_5	SO_3	Cl	K_2O	CaO
W1	~	0.168	1.16	19.2	39.3	0.395	0.229	0.0062	1.08	2.08
W2	~	0.0698	1.64	19.2	23.9	0.179	0.0536	0.0157	0.612	0.642
W3	~	0.0324	0.768	3.24	5.38	0.187	0.0779	0.0133	0.281	1.64
W4	~	0.335	0.871	25.9	53.1	0.251	0.267	~	2.00	1.18
W5	0.550	0.302	0.942	25.6	56.9	0.231	0.379	0.0097	1.48	0.904
	TiO_2	V_2O_5	Cr_2O_3	MnO	Fe_2O_3	Co_2O_3	NiO	CuO	ZnO	Ga_2O_3
W1	0.898	0.0395	0.0177	1.11	34.0	~	0.0069	0.119	0.0249	~
W2	0.792	0.0275	0.0241	0.315	52.3	0.0206	0.0337	0.0364	0.0461	0.0068
W3	0.0826	~	~	3.08	84.9	~	0.0298	0.150	0.0314	~
W4	1.34	~	0.0225	0.121	14.3	~	0.0091	0.0136	0.0150	0.0072
W5	1.25	~	0.0152	0.103	11.1	~	0.0072	0.0196	0.0074	0.0046
	Rb_2O	As_2O_3	Rb_2O	SrO	Y_2O_3	ZrO_2	Nb_2O_5	MoO_3	BaO	PbO
W1	0.0054	~	~	0.0586	0.0095	0.0326	0.0026	~	0.0516	0.0070
W2	~	~	~	0.0163	0.0075	0.0275	0.0031	~	0.0961	0.0085
W3	~	~	~	0.0055	0.0048	0.0029	~	0.0038	0.0649	0.0126
W4	0.0111	~	~	0.0706	0.0087	0.0519	0.0038	~	0.0726	~
W5	~	0.0038	0.0076	0.0807	0.0062	0.0369	0.0030	~	0.0546	~

Based on the XRF analysis results of the slag, the main components of the slag sample are SiO_2, Al_2O_3, as well as Fe_2O_3. According to the standards for identifying ironmaking slag, the CuO content in the five slag samples ranges between 0.0136% and 0.119%, which is far below the CuO standard value of 0.5% found in non-ferrous smelting slag. Additionally, the Pb and Zn contents are both below 0.1%, and the samples do not contain Ag or other non-ferrous metal elements, which aligns with the criteria for ancient ironmaking slag. Based on this, it can be concluded that these five slag samples are from ancient ironmaking site. the SiO_2 content in the slag samples ranges from 23.9% to 56.9%, Al_2O_3 content ranges from 19.2% to 25.9%, and CaO content ranges from 0.642% to 2.08%. the slag's basicity is between 0.0159 and 0.3048. the samples are clearly high-silica slag, indicating that no lime or other fluxing agents were added during the ironmaking process.

Through scanning electron microscopy (SEM) and energy dispersive spectroscopy (EDS) analysis of the slag sample's matrix, as shown in Figure 7, it was determined that the matrix structure is primarily composed of fayalite (iron olivine), with some spinel and a small amount of glassy silicates present.

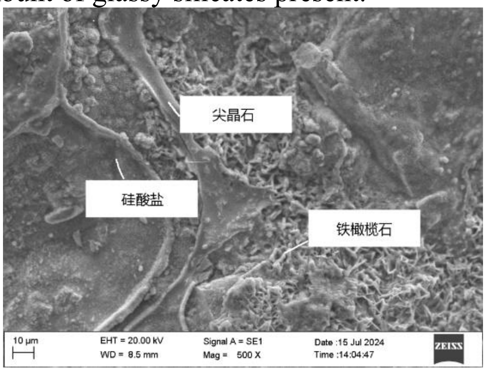

Figure 7. SEM and EDS Analysis Results of the Slag Sample

The combined content of Fe_2O_3, Al_2O_3, and SiO_2 in the five slag samples is close to 94%. Therefore, the FeO-Al_2O_3-SiO_2 ternary phase diagram can be used to determine the softening temperature of the slag. As shown in Figure 8, the compositions of the five slag samples, labeled W1 to W2, correspond to the △ region in the diagram. Based on this, the softening temperature range of the slag is determined and listed in Table 3.

Table 3. Converted Softening Temperature Ranges for the Five Slag Samples

	FeO(%)	SiO_2(%)	Al_2O_3(%)	temperature(℃)
W1	30.6	39.3	19.2	1250~1500
W2	47.07	23.9	19.2	1310~1480
W3	76.41	5.38	3.24	1163~1530
W4	12.87	53.1	25.9	1500~1650
W5	9.99	56.9	25.6	1530~1670

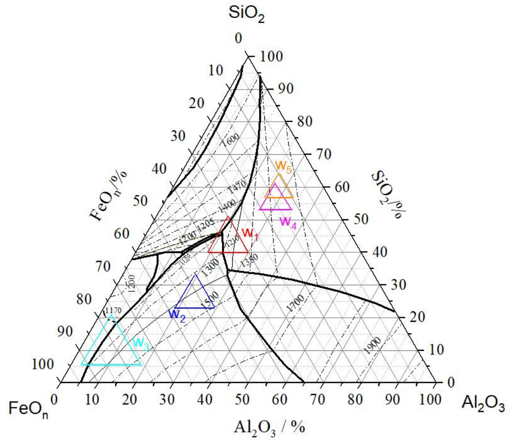

Figure 8. Softening Temperature Range of the Slag Sample in Wangguan Historical Site

2.3 Composition Analysis of Iron Farming Tools in Ming Dynasty

Non-destructive XRF testing was conducted on the Ming dynasty iron farming tools unearthed from the Wangguan site and currently housed in Benxi Museum. the relevant composition are presented in Table 4. Samples T1-T2 are Ming dynasty shovels, samples T3-T6 are hoes (with T3-T4 being hoe blades and T5-T6 being hoe hoops), samples T7-T9 are sickles (with T7-T8 being sickle hoops and T9 being the sickle blade), and samples T10-T13 are choppers (with T10, T11, and T13 being the back of the chopper and T12 being the chopper blade). It is important to note that due to the need to test the unrusted parts of the tools, there are some differences in the chemical composition at different test points of the same tool. Additionally, the handheld XRF device cannot measure the carbon content in the tools.

Table 4. XRF Analysis Results of Iron Farming Tools of Ming Dynasty Found in Wangguan Historical Site

	Fe	Si	Al	Mg	P	Co	Pb	Ti	Zn	Mn
T1	83.22	12.03	2.87	<0.455	1.41	<0.022	0.231	0.137	<0.003	~
T2	82.73	12.28	2.83	<0.436	1.42	<0.021	0.264	0.382	<0.002	~
T3	80.67	13.02	3.56	<0.438	1.63	<0.020	~	<0.015	<0.002	<0.005
T4	81.28	12.53	3.81	<0.426	1.25	<0.020	~	<0.015	<0.002	~
T5	89.53	8.77	1.09	0.491	0.21	0.024	~	0.049	~	~
T6	98.92	0.598	0.116	0.519	0.055	~	~	~	~	~
T7	73.54	19.58	4.05	0.461	0.86	0.02	~	0.099	0.002	0.005

Academic Education Publishing House

T8	75.55	18	3.12	0.56	1.44	0.023	0.017	0.072	0.002	0.005
T9	83.58	11.53	3.35	0.438	0.729	0.02	~	~	~	~
T10	95.24	3.53	0.116	0.568	0.185	~	~	~	~	~
T11	93.89	4.18	0.625	0.546	0.685	0.024	~	~	~	~
T12	81.47	14.41	2.75	0.434	0.226	0.022	0.04	0.099	~	~
T13	95.61	3.56	0.116	0.48	0.072	0.023	~	~	~	~
	Cr	**Ni**	**Cu**	**V**	**Zr**	**Mo**	**Y**	**Nb**	**S**	
T1	0.041	0.021	0.020	0.012	<0.001	0.005	<0.001	0.0038	<0.014	
T2	0.044	0.018	0.018	0.015	<0.001	0.004	<0.001	0.003	<0.015	
T3	0.043	0.013	0.018	~	<0.001	~	<0.001	0.003	0.267	
T4	0.050	~	0.020	~	<0.001	0.002	<0.001	0.002	0.272	
T5	0.053	0.019	0.013	~	0.001	~	0.001	0.004	1.05	
T6	0.04	~	~	~	~	~	~	0.003	1.06	
T7	0.046	0.028	0.025	~	0.001	~	0.001	0.003	0.734	
T8	0.037	0.026	0.018	~	0.001	~	0.001	0.004	0.72	
T9	0.049	~	0.017	~	~	~	~	0.002	1.78	
T10	0.052	~	0.019	~	~	0.003	~	0.004	0.853	
T11	0.048	~	0.019	~	0.001	0.003	~	0.005	0.904	
T12	0.042	0.025	0.021	~	0.001	~	0.001	0.003	0.549	
T13	0.049	~	0.019	~	~	~	~	0.003	0.576	

2.4 Composition Analysis of Crucibles

Measurements of the collected crucible fragment samples revealed that all fragments were either arc-shaped (crucible wall) or circular (crucible bottom), with the bottom having a maximum diameter of 15 cm and the crucible wall being approximately 2 cm thick. A comparison between the crucible fragment samples shown in Figure 4 and the intact crucible from Benxi museum shown in Figure 5 confirms that the fragments match the shape of the complete crucible. Actual measurements of the intact Ming dynasty crucible determined it to be a spindle-shaped container with a height of 30 cm, a bottom diameter of 15 cm, and a maximum belly diameter of 17 cm. the calculated volume of the crucible is approximately 5300 cm^3. Two sets of crucible fragment samples, G1 and G2, were crushed using a jaw crusher, and then homogenized and sampled. the comprehensive XRF composition analysis results are presented in Table 5.

Table 5. Comprehensive Composition Analysis of Crucibles

	F	**Na_2O**	**MgO**	**Al_2O_3**	**SiO_2**	**P_2O_5**	**SO_3**	**Cl**	**K_2O**
G1	~	0.157	0.548	35.2	47.4	0.177	0.162	0.0068	1.99
G2	0.522	0.234	0.785	21.6	60.2	0.113	0.681	0.0459	2.19
	CaO	**TiO_2**	**V_2O_5**	**Cr_2O_3**	**MnO**	**Fe_2O_3**	**Co_2O_3**	**NiO**	**CuO**
G1	0.628	1.83	~	0.0332	0.187	11.4	0.0116	0.0125	0.0134
G2	1.40	1.58	0.0462	0.0192	0.149	10.3	~	0.0093	0.0098
	ZnO	**Ga_2O_3**	**Rb_2O**	**As_2O_3**	**SrO**	**Y_2O_3**	**ZrO_2**	**Nb_2O_5**	**BaO**
G1	0.0275	0.0067	0.0109	0.0062	0.0212	0.0078	0.0643	0.0069	0.0789
G2	0.0178	0.0056	0.0142	0.0034	0.0211	0.0057	0.0478	0.0044	~

As seen in Table 5, the primary components of the crucible are SiO_2, Al_2O_3 and Fe_2O_3, with SiO_2 and Al_2O_3 accounting for over 81% of the composition. Based on the scanning electron microscopy analysis of the crucible fragments shown in Figure 8, the crucible matrix is primarily composed of SiO_2 and Al_2O_3. the presence of Fe_2O_3 in the comprehensive analysis is likely due to slag adhering to the crucible during the smelting process, rather than being part of the original refractory matrix. After converting the Al_2O_3 and SiO_2 content in the crucible composition, the values were plotted onto the Al_2O_3-SiO_2 binary phase diagram, as shown in Figure 10. Additionally, according to the classification of refractory materials, the crucible is categorized as a semi-siliceous, semi-acidic aluminosilicate refractory. Mineralogical analysis using a polarizing microscope indicates that the main mineral phases are quartz polymorphs, mullite ($3Al_2O_3 \cdot 2SiO_2$), and some glassy phases. Based on the analysis in Figure 10, the Al_2O_3/SiO_2 ratio of the crucible ranges between 0.35 and 0.74, allowing the determination that the crucible's refractory temperature is between 1710 °C and 1800 °C.

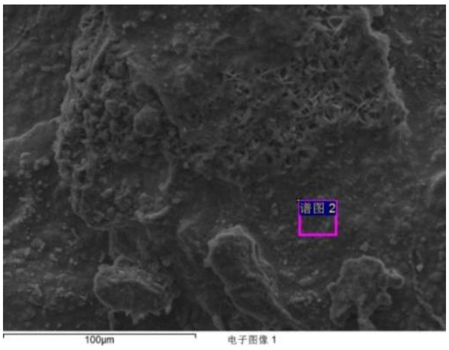

Figure 9. SEM Analysis of Crucible

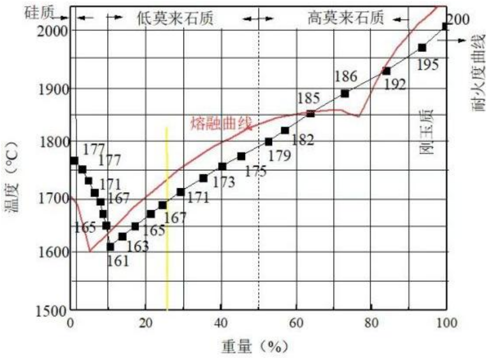

Figure 10. Refractoriness Analysis of Crucible

According to modern refractory material theories, aluminosilicate refractories are not suitable for use in reducing atmospheres, and the lower the Al_2O_3/SiO_2 ratio, the weaker the material's resistance to iron oxide erosion. Therefore, when the Al_2O_3/SiO_2 ratio is low, the iron oxide content in the refractory should be kept as low as possible to ensure the crucible's integrity. As shown in Table 2, the crucibles from Wangguan site in Benxi have a low Al_2O_3/SiO_2 ratio and contain a significant amount of iron oxide, suggesting that the service life of these crucibles in the furnace would have been relatively short. This makes the intact crucible exhibited at Benxi Museum particularly rare and valuable.

3 Analysis and Discussion

The Ming dynasty Wangguan ironmaking site in Benxi has yielded a rich collection of metallurgical artifacts, including slag, crucibles, and unearthed iron farming tools. This site provides relatively complete evidence of ironmaking technology from Ming dynasty, including metallurgical reactors and slag-metal biphasic products. By applying modern metallurgical principles to study the relationships between slag, metal, and the crucible reactors used, new insights can be gained into the origins of ancient ironmaking in northeastern China, particularly in Benxi region, thus offering valuable reference points for understanding the development of this significant aspect of civilization.

3.1 Calculation Analysis and Validation of Smelting Temperature

In the ironmaking process, the presence of sulfur in slag and metal allows for the establishment of a connection between slag and metal based on the distribution of sulfur. According to metallurgical principles, it is theoretically feasible to calculate the sulfur distribution ratio between slag and metal and, in turn, back-calculate the smelting temperature. Tamura et al. correlated the sulfur distribution coefficient Ls in the ironmaking process with operating parameters. Starting from the basic reaction $0.5S_{2(g)} = [S]$ and defining the slag's sulfur absorption index as $C_s = (S)(P_{O2}/P_{S2})^{0.5}$, the authors derived an expression for the equilibrium distribution coefficient of sulfur as follows.

$$L_S = (S)/[S] = \exp\left(0.263[C] + 0.145[Si] - 0.06[Mn] + 2.303\lg C_S - \frac{3076}{T} + 13.56\right)/P_{CO} \quad (1)$$

Based on the distribution reaction of sulfur between slag and metal phases, from an equilibrium perspective, an exact quantitative expression for the sulfur distribution coefficient Ls can be further derived as

$$L_S = \exp\left[11.27 + 2.602R - 19649/T + 2.303\sum_i e_S^{(i)}[i] - lnP_b\right] \quad (2)$$

where R, T and P_b are the binary basicity, smelting temperature and blast pressure, respectively. $i = S, C, Mn, P, V, Al, Mg, Ti, Si\ldots$ the interactive coefficient $e_S^{(i)}$ is listed in Table 6 from Ref. [24].

Table 6. Interactive Coefficient of Sulfur in Iron

	S	Al	C	Co	Cr	Mg	Mn	Cu
$e_S^{(i)}$	-0.028	0.035	0.11	0.0026	-0.011	0.038	-0.026	-0.0084
	Nb	Si	Zr	Ti	V	Si	P	
$e_S^{(i)}$	-0.013	0.063	-0.052	-0.072	-0.016	0.065	0.029	

It is important to note that while both the slag samples and the iron farming tools originate from the same site, it cannot be confirmed that they were produced in the same smelting operation, meaning that there is no one-to-one correspondence between the slag samples and the iron tools. Therefore, it is necessary to pair the sulfur content of all slag samples with the sulfur content of the iron tools to create corresponding combinations. This approach yields 65 sets of slag-metal distribution ratio Ls data, as presented in Table 7.

Based on Table 7, the sulfur content in tools T1 and T2 is relatively low. Considering the three key factors influencing desulfurization in ironmaking process—high temperature, high basicity, and a reducing atmosphere—it can be inferred that although no flux was used during

Academic Education Publishing House
- A E P H -

the smelting process, the relatively high temperature or the stronger reducing atmosphere may have led to a higher Ls (sulfur distribution coefficient). This resulted in relatively high desulfurization efficiency. In modern blast furnace ironmaking, where it is easier to obtain high temperatures, high basicity, and a reducing atmosphere, Ls values typically range from 30 to 50, allowing the sulfur content in hot metal to be controlled below 0.07%. the sulfur content in the shovels (T1 and T2) is even lower than that found in modern blast furnace hot metal, suggesting that additional external processes, such as forging, were likely employed during the production of these tools. These processes would have provided special treatment, enabling the production of shovels with a certain strength and relatively thin blades. the specific processing techniques warrant further investigation. In contrast to T1 and T2, the sulfur content in tools T3 to T6 ranges from 1.05% to 1.72%, with Ls values between 0.02 and 0.5678. the higher sulfur content resulted in the production of thicker, heavier hoes.

Table 7. L_S Values for Slag and Iron Samples

	W1	W2	W3	W4	W5
T1	6.543	1.5314	2.226	7.629	10.114
T2	6.107	1.429	2.077	7.12	10.107
T3	0.3431	0.0803	0.1167	0.4	0.5678
T4	0.3368	0.0788	0.1145	0.3926	0.5574
T5	0.087	0.02	0.0296	0.102	0.144
T6	0.086	0.02	0.029	0.101	0.143
T7	0.3368	0.0788	0.1145	0.3926	0.5574
T8	0.1272	0.0298	0.0433	0.1483	0.2106
T9	0.0514	0.012	0.0175	0.06	0.0852
T10	0.1074	0.0251	0.0365	0.1252	0.1777
T11	0.1013	0.0237	0.0345	0.1181	0.1676
T12	0.1668	0.0391	0.0568	0.1945	0.2761
T13	0.1590	0.0372	0.0541	0.1854	0.2632

Since the handheld XRF ore element analyzer cannot measure the carbon content in the iron tools, equation (2) involves both temperature and carbon content as unknown variables. To accurately calculate the carbon content, it is necessary to use other relationships between temperature and carbon content. When liquid iron forms a multi-element alloy by dissolving other elements, the saturation carbon content is influenced by the content of the dissolved elements. J. F. Elliot et al. summarized the relationship between these factors, including the effect of temperature, into the following empirical equation:

$$[\%C] = 1.34 + 2.54 \times 10^{-3}t - 0.35[P] + 0.17[Ti] - 0.54[S] + 0.04[Mn] - 0.30[Si] \quad (3)$$

By solving equations (2) and (3) simultaneously, the temperature and carbon content can be determined. the solution process is illustrated in Figure 11, where the intersection points of the straight-line T(C) and the curves T1-W1~T1-W5 correspond to the horizontal and vertical coordinates, which represent the smelting temperature and carbon content of the iron farming tool under the corresponding slag composition during the ironmaking process. This method yields 65 corresponding sets of temperature and carbon content data, as shown in Table 8.

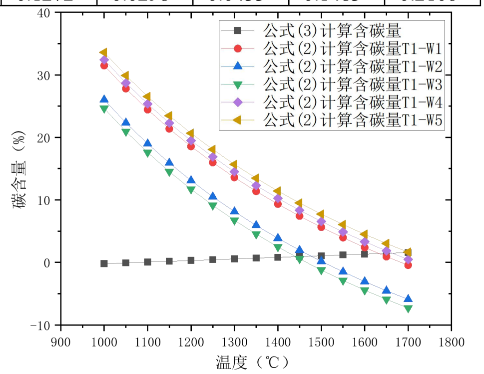

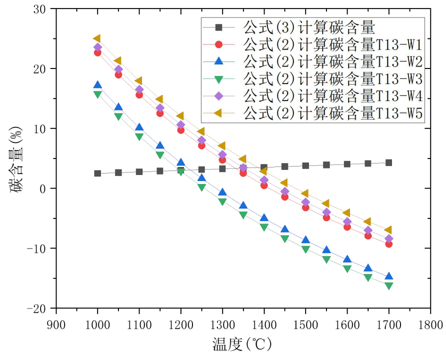

Figure 11. Relationship Between Carbon Content in Farming Tools and Smelting Temperature

Table 8. Relationship Between the Smelting Temperature and Carbon Content of the Farming Tools Determined by Equations (2) and (3)

	W1		W2		W3		W4		W5	
	t(℃)	[%C]	t(℃)	[%C]	t(℃)	[%C]	t(℃)	[%C]	t(℃)	[%C]
T1	1643	1.3890	1478	0.9988	1441	0.9309	1663	1.4742	1703	1.5421
T2	1628	1.3554	1472	0.9649	1437	0.8800	1658	1.4403	1703	1.5591
T3	1212	- 0.6239	1118	- 0.8531	1098	- 0.9550	1230	- 0.5985	1259	- 0.5475
T4	1210	- 0.3679	1120	- 0.5885	1095	- 0.6735	1230	- 0.3141	1259	- 0.2122
T5	1358	1.9439	1248	1.6570	1222	1.5959	1380	2.0051	1416	2.0866
T6	1419	4.5812	1297	4.2756	1267	4.2105	1443	4.6491	1479	4.7538

T7	1140	-2.8709	1056	-3.0865	1040	-3.1477	1155	-2.8523	1179	-2.7809
T8	1156	-2.5846	1071	-2.7612	1051	-2.7883	1170	-2.5008	1194	-2.4624
T9	1325	0.8523	1217	0.5772	1193	0.5178	1345	0.8930	1378	0.9949
T10	1298	3.0390	1196	2.7929	1170	2.7349	1317	3.0985	1348	3.1834
T11	1329	2.9400	1221	2.6584	1196	2.5806	1350	2.9641	1382	3.0560
T12	1218	-0.4397	1127	-0.6757	1104	-0.7165	1235	-0.3905	1265	-0.3294
T13	1332	3.3447	1222	3.0730	1198	2.9881	1350	3.4041	1386	3.4819

In the calculation of the relationship between the farming tools and slag using equations (2) and (3), three main constraints must be considered and they are (1) the calculated carbon content must be greater than 0, (2) the calculated temperature must be greater than or equal to the corresponding slag softening temperature, (3) the calculated temperature must not exceed the refractoriness of the crucible. As shown in Table 8, any corresponding relationship where $[\%C] \le 0$ is clearly unreasonable, indicating that the slag-metal composition cannot form a valid correlation. Additionally, the relationship is further constrained by the conditions in Table 3—if the temperature does not fall within the softening temperature range specified in Table 3, a valid slag-metal correspondence cannot be established. Lastly, if the smelting temperature exceeds the refractoriness of the crucible as determined from Figure 10, that group also cannot form a valid slag-metal correspondence. Based on the analysis above, after removing the incompatible entries, a total of 14 valid slag-metal corresponding relationships were obtained: T1-W2, T1-W3, T2-W2, T2-W3, T5-W1, T5-W5, T6-W1, T6-W2, T6-W4, T6-W5, T9-W1, T10-W1, T11-W1, and T13-W1. These relationships indicate that the slag compositions are compatible with the smelting conditions for producing the corresponding iron for making the farming tools. Therefore, these specific slag samples can be considered the slag produced during the ironmaking process.

The study also revealed an important phenomenon: when matching the same farming tool, the results varied significantly depending on the test point. For example, tools T3, T4, T7, T8, and T12 all correspond to the blade sections of the tools, and in each of these cases, the sulfur content in the blade was lower than in other parts of the tool. This indicates that the chemical composition of the blade sections could not be matched with any of the existing slag compositions. This suggests that after obtaining molten iron, the blades underwent additional processing, such as forging, during the manufacturing of the tools, which altered the chemical composition of the blade sections.

3.2 Inference of Fuel and Reducing Agent for Smelting

According to *Tiangong Kaiwu*, "Coal is found all over the world and is used solely for forging and smelting metals and minerals... " There are records from Han dynasty indicating that the Benxi Lake area used "charcoal to heat stoves". Furthermore, during Sui, Tang, Liao, and Jin dynasties, there were continuous records of coal mining activities, suggesting that coal production in this region has been uninterrupted since ancient times. the history of Liao Dynasty (Biography of Yelü Yuzhi) records that during the reign of Emperor Taizong of Liao, Yelü Deguang (927–947 AD), "the land around Liangshui (Taizi River) is fertile and rich, with abundant resources of wood, iron, salt, and fish. " Additionally, during the coal production process by the modern Benxi lake coal and iron company, remnants of coal mining activities from Ming and Qing dynasties were frequently discovered. Unlike the almost sulfur-free slag found at other smelting sites, the slag samples collected in this study contain sulfur levels ranging from 0.0779% to 0.379%, and the sulfur content in the iron farming tools ranges from 0.014% to 1.78%. Given that the iron ore in Benxi region is characterized by low sulfur and low phosphorus, and that no fluxes like lime were added during the smelting process (as indicated by the slag composition analysis), the only source of sulfur in both the slag and metal can be attributed to the reducing agent or fuel used. Given the historical abundance of both iron ore and coal resources in Benxi region, and considering that the sulfur content in locally produced coal ranges from 0.92% to 2.90%, significantly higher than in other coal-producing areas in China, it can be further inferred that coal was likely used extensively in the ironmaking process in Benxi from an early period.

3.3 Inference of Smelting Process

According to Ref. [33], ancient iron production methods in China can be broadly categorized into two types. the first type uses charcoal or roughly burned wood as both fuel and reducing agent, which is added to the furnace along with iron ore without the use of flux. the furnace design is similar to modern blast furnaces, featuring a slag-iron outlet and a tuyere, with bellows or waterwheels used to elevate pressure. the second type is the Shanxi method, which involves mixing smokeless coal with iron ore and placing the mixture into clay crucibles. Dozens of these crucibles are then loaded into a rectangular furnace, where they are heated with coal. the iron ore is reduced and melted inside the crucibles, and each crucible yields a single block of iron that can be cast into agricultural tools like plowshares. the crucible fragments collected in this study, along with the complete Ming dynasty crucibles exhibited at Benxi Museum, suggest that the smelting method at Wangguan site clearly belongs to the latter category. As for whether Wangguan site employed enhanced smelting technology like forced air blowing, this remains uncertain due to the lack of physical evidence and related records in Benxi region. However, it is possible to hypothesize based on theoretical considerations.

$$P = P_0 \frac{V^2}{g} \tag{4}$$

where P, P0, V and g are the blast pressure, pressure at sea level, blast velocity as well as gravitational acceleration, respectively. By substituting blast velocity into equation (4), the blast pressure can be obtained. Then, by applying the blast pressure into equation (2), the smelting temperatures corresponding to the 14 slag-metal relationships discussed in Section 3.1 can be determined. the results are presented in Table 9.

Table 9. Smelting Temperatures Calculated under Different Blast Velocities

	3.132 (1.0)	3.209 (1.05)	3.285 (1.1)	3.359 (1.15)	3.431 (1.2)	3.571 (1.3)	3.706 (1.40	3.836 (1.5)	3.962 (1.6)	4.429 (2.0)
T1-W2	1478	1483	1487	1490	1499	1503	1515	1520	1525	1556
T1-W3	1441	1447	1450	1453	1459	1467	1474	1484	1493	1515
T2-W2	1472	1476	1480	1485	1489	1501	1509	1515	1520	1547
T2-W3	1437	1441	1445	1449	1453	1463	1471	1476	1482	1509
T5-W1	1358	1363	1369	1371	1376	1382	1390	1396	1401	1421
T5-W5	1416	1419	1424	1430	1434	1440	1448	1456	1461	1482
T6-W1	1419	1424	1428	1433	1437	1446	1451	1457	1464	1491
T6-W2	1297	1300	1304	1308	1312	1321	1326	1331	1334	1353
T6-W4	1443	1447	1451	1456	1460	1469	1478	1483	1493	1513
T6-W5	1479	1484	1489	1493	1498	1508	1515	1521	1528	1554
T9-W1	1325	1329	1333	1337	1340	1348	1355	1361	1366	1387
T10-W1	1298	1302	1306	1309	1313	1319	1325	1331	1337	1356
T11-W1	1329	1333	1337	1341	1344	1350	1357	1363	1371	1388
T13-W1	1332	1335	1339	1343	1347	1352	1362	1366	1376	1394

As shown in Table 9, when the blast pressure is doubled, the blast velocity increases from 3.132 m/s to 4.429 m/s, the smelting temperature rises by 56°C to 78°C. This temperature increase is sufficient to meet the softening temperature range of the Wangguan slag samples while remaining below the refractoriness of the crucible. Therefore, it can be inferred that blast operations were likely used in the ironmaking process at Benxi in Ming dynasty. the specific form of the blast operation, however, requires further investigation.

4. Conclusions

The Wangguan ironmaking site in Benxi was the location of an ironworks under the jurisdiction of a "Baihu Office" (a military administrative unit) in sortheastern China in Ming dynasty. the site's well-preserved metallurgical evidence, including slag, metal artifacts, and reactors, provides a comprehensive chain of evidence that offers new scientific data for studying ironmaking technology in northeastern China in Ming dynasty.

Through the analysis of the ternary phase diagram of Ming dynasty ironmaking slag from Benxi region, the slag-metal sulfur distribution ratio, and the quantitative analysis of the relationship between carbon content and temperature in iron products, a matching relationship between iron products and slag can be established. This provides a novel analytical method for the investigation of ancient ironmaking technology. the conclusions drawn from this method demonstrate that it is feasible to establish a large database of ancient slag and iron compositions and to infer the smelting process based on the distribution patterns of elements between slag and metal.

The slag from the Ming dynasty ironmaking site in Benxi is acidic and high in silica, with no lime or other fluxing agents added. the material of the ironmaking crucibles is semi-siliceous and semi-acidic aluminosilicate, with refractoriness exceeding 1650°C, which was sufficient to meet the iron smelting requirements of that time.

The ironmaking process at Benxi region in Ming dynasty used coal as a reducing agent without adding lime or other fluxing agents, which resulted in generally higher sulfur content in the iron farming tools. However, for thinner tools or the blade sections of tools, post-processing techniques such as forging were likely applied to reduce the sulfur content. This indirectly demonstrates that the ironworkers at Benxi region in Ming dynasty had already harnessed techniques for controlling the sulfur content in iron products.

Based on the calculations of blast pressure and smelting temperature, it can be inferred that the ironmaking process at Benxi region in Ming dynasty widely utilized bellows for blast operations.

Acknowledgments

Basic Research Project of Education Department of Liaoning Province, “Applied Research on Improving Concentrate Ratio through Sintering Ore Mixing” (No. 2024JYTKYTD-16).

Project: Key R&D Project of Liaoning Province 2020JH2/10100019, Project of Liaoning Provincial Department of Education 2024JYTKYTD-17, W20171kyqn-09.

Author Bio: Huang Yan (1979~), female, doctoral student, associate professor, email: yanyan0303@163. com; Research direction: Ancient metallurgical history.

Corresponding author: Chen Ren (1970~), male, Doctor of Engineering, Professor Email: toughold@163. com; Research direction: Metallurgical Reaction Engineering and Resource Comprehensive Utilization.

References

[1] Huang Xing, Qian Wei. Research on the Type of Iron Smelting Shaft Furnace in Ancient China, Science Press, 2022.01 p1-2.

[2] Collection of Research on the Origin of Chinese Metallurgical Iron, Qilu Publishing House, 2012.07, p1-5.

[3] Huang Quanshen, Li Yanxiang, Chen Jianli, Tie Fude, Research and Exploration of Ancient Ironmaking Technology Based on Slag Analysis, Cultural relics technology.

[4] Yang Ju, Li Yanxiang, Yu Pu. Scientific analysis of ironware unearthed from Hujiaying site in Yanqing, Beijing [J]. Journal of Guangxi University for Nationalities (Natural Science Edition), 2014, 20(01):37-43.

[5] Liu Haifeng, Chen Jianjian, Mei Jianjun, Shi Lei, Jia Jinbiao. Experimental study on the iron artifacts unearthed from the Dongheishan Site in Xushui, Hebei [J]. Southern cultural relics, 2013(01):133-142.

[6] Wenjuan. Analysis of iron artifacts unearthed from the Mogou site and preliminary study of iron smelting technology [D]. Northwest University, 2015.

[7] Tan Jian, Li Yanxiang. Experimental Study on Iron Objects Unearthed from Fenglin Ancient City, Heilongjiang Province [J]. Chinese Cultural Relics Science Research, 2015(01):64-66.

[8] Chen Jianjian, Han Ruyi, Wan Xin, Li Yanxiang. Metallographic Experimental Study on Iron Objects Unearthed from Lama Cave Cemetery in Beipiao [J]. Cultural Relics, 2001(12):71-79+1.

[9] Yu Heyin. Report of Benxi Lake Coal and Iron Company [R]. Ministry of Agriculture and Commerce, Department of Mines, 1926.156.

[10] Jia Ying, Li Xinquan, Liang Zhilong. Preliminary Study on Metallography of Goguryeo Ironware in Wunvshancheng [J]. Protection of Cultural Relics and Archaeological Science, 2007, 19(3):16-25.

[11] Guo Meiling, Chen Kunlong, An Wenrong, Li Ruizhe. Preliminary scientific analysis of iron artifacts unearthed from the tomb area under the mountain city of the Ji 'an Donggou ancient tomb group [J]. Northern Cultural Relics, 2021(02):57-67.

[12] Jiang Jihao. Research on ironware and iron smelting remains unearthed from the

southeast site of Beitou, Ji 'an, Jilin [D]. Beijing University of Science and Technology, 2022.
[13] Wang Zhixi, A brief history of China 's modern ironmaking industry, Ironmaking, 1986, 5(4):1-4.
[14] Huang Quansheng, Li Yanxiang. Chen Jianli. Revealing the research and exploration of ancient ironmaking technology based on slag analysis. Cultural Relics Technology, 2016.11 P145-153.
[15] Huang Quansheng, Huang Qianxi, Zou Guisen, Li Yanxiang, Chen Jianjian. Preliminary Study on the Ancient Metallurgical Site of Chuanbutielu Village, Luoding, Guangdong Non-ferrous Metals (Smelting Part), 2023.03, P139-P148.
[16] Huang Quansheng, Li Yanxiang, Chen Jianjian, Tie Fude. Research and exploration of ancient ironmaking technology based on slag analysis [J]. National Museum of China, 2016(11):145-153.
[17] Wei Guofeng, Qin Ying, Han Chuwen, Qu Yi, Wang Changsui, Dong Yawei. Analysis of mining and metallurgical relics from Daye Li Degui smelting site [J]. Rock and ore test, 2008(02):99-102.
[18] Chen Jianjian, Han Ruyi, Saito Nu, Jincun Fengxiong. the development of ironware and iron-smelting industry in ancient Northeast China from the perspective of metallography of ironware [J]. Northern cultural relics, 2005(01):17-28+115-116.
[19] Chen Jianli. A new exploration of ancient Chinese metal smelting civilization [M]. Beijing: Science Press, 2014.03:339-340.
[20] Li Nan, Gu Huazhi, Zhao Huizhong. Refractory Material, Science Metallurgical Industry Press, 2010.07 P139-P143.
[21] Chen Min, Yu Jingkun, Wang Nan. Refractory and Fuel Burning, Northeastern University Press, 2005.12, the first edition, P56-P62.
[22] Yang Guiping, Xie Yusheng, Zhang Heng, Zhang Hongping. Determination of distribution coefficient of sulfur between slag and iron in blast furnace smelting process, Journal of Iron and Steel Research, VOL. 1, No. 4, Nov. 1989.
[23] Keiji Tamura, Katsuya Axe, Nobunao Nishida, Tetsudo Steel. 67(1981), 2641.
[25] Wang Xiaoliu. Iron and Steel Metallurgy, Metallurgy Industry Press, P163.
[26] Yang Weizeng. Tiangong Kaiwu [M]. Beijing: Zhonghua Book Company, 2023.05 P308-P313.
[27] kangkuolin, On the development of coal resources in Benxi area.
[28] Yang Kuan. A brief history of the development of iron and copper smelting technology in China [M]. Shanghai: Shanghai People 's Publishing House, 1960.02.
[29] Gao Linsheng, Yang Fu, et al. the History of Ancient Chinese Steel [M]. Beijing: Zhonghua Book Company, 1962.06.
[30] Chen Jianli, Mao Ruilin, Wang Hui, Chen Honghai, Xie Yan, Qian Yaopeng. the ironware unearthed from the tombs of Mogousiwa Culture in Lintan, Gansu and the origin of iron smelting technology in China [J]. Relics, 2012(08):45-53+2.
[31] Sun Jinji. the history of the use of ironware by ancient ethnic groups in Northeast China and their views on the ' Iron Age ' [J]. Ethnological research, 1984.